14TH CANADIAN MASONRY SYMPOSIUM
MONTREAL, CANADA
MAY 16TH – MAY 20TH, 2021

EVALUATING DAMAGE OF A CONTROLLED ROCKING MASONRY WALL WITH SUPPLEMENTAL ENERGY DISSIPATION

East, Matthew[1]; Ezzeldin, Mohamed[2] and Wiebe, Lydell[3]

ABSTRACT

Controlled rocking systems have been used in numerous structures around the world as a seismic force resisting system. In a controlled rocking wall system, the wall is allowed to uplift from the foundation during seismic events, reducing its lateral stiffness and minimizing the seismic force demands. This rocking response is controlled using post-tensioning and/or supplemental energy dissipation. In this way, controlled rocking walls are designed to have less damage than conventional systems and to have negligible residual deformations. Promising strides have been taken to apply the concept of controlled rocking systems to masonry walls; however, several issues have been encountered due to the low strength and brittle nature of the masonry material in compression. In addition, there are many challenges with the numerical modeling of controlled rocking masonry walls (CRMWs) due to the variability of the material and the anisotropic nature of the systems they form. The current paper develops and validates a numerical model to capture the performance of CRMWs. The wall arrangement considered herein omits post-tensioning and maintains the footprint of a conventional reinforced masonry shear wall, while also providing enough space to install replaceable energy dissipation devices to address the low inherent damping of CRMWs. First, the model has been validated based on experimental tests in previous studies of other walls and energy dissipation components. The model is then used to evaluate a damage index, adapted from damage modeling of reinforced concrete components. Finally, the validated model is used to analyze a 2-storey CRMW in order to evaluate the amount of damage compared to that of a conventional reinforced masonry shear wall.

KEYWORDS: *seismic design, controlled rocking, reinforced masonry, shear walls, numerical modelling*

[1] PhD Candidate, Department of Civil Engineering, McMaster University, Hamilton, ON, L8S 4L7, Canada, eastma@mcmaster.ca
[2] Assistant Professor, Department of Civil Engineering, McMaster University, Hamilton, ON, L8S 4L7, Canada, ezzeldms@mcmaster.ca
[3] Associate Professor, Department of Civil Engineering, McMaster University, Hamilton, ON, L8S 4L7, Canada, wiebel@mcmaster.ca

INTRODUCTION

Masonry is one of the world's oldest construction materials and is still used extensively for low- to mid-rise residential, commercial, and industrial structures. However, modern seismic design requirements have significantly affected the practicality of masonry structures as they are considered considerably less ductile than their counterparts constructed from reinforced concrete or steel, and thus more vulnerable during seismic events. The seismic vulnerability of masonry structures has been observed in many earthquakes recently, notably Northridge in 1994 [1] and Christchurch in 2011 [2]. A design concept that has been recently investigated to mitigate such a vulnerability is the use of self-centering structures with rocking as the primary mode of deformation, as opposed to typical shear- and flexurally-dominated deformations [3]. Adopting such a design concept to masonry walls is expected to allow them to have less damage than conventional masonry walls and to have also almost zero residual deformations. In a controlled rocking masonry wall (CRMW) system, the wall is unbonded from the foundation and subsequently is allowed to uplift from the foundation during seismic events. Alongside the development and improvement of controlled rocking as a viable alternative to conventional seismic force resisting systems comes the need for accurate means to numerically capture the response of such systems.

Several research studies have applied the concept of controlled rocking to masonry walls, such as Laursen & Ingham [4] and Rosenboom & Kowalsky [5]. These studies relied on post-tensioning tendons that were placed through the walls in order to provide restoring forces, thus allowing the wall to return to its original vertical alignment following a seismic event. Specifically, when a wall is under in-plane lateral loading that represents a seismic event, a single major crack forms at the wall-foundation interface. By further increasing this in-plane loading, the wall uplifts from the foundation, resulting in a displaced shape that is characterized by rotation about the rocking toe. When the load is released after the seismic event, the post-tensioning tendons return the wall to its initial position, provided that they still have sufficient post-tensioning forces despite any inelastic strains [6].

Experimental tests have indicated that a self-centering ability can be achieved by CRMWs and the extent of damage can be localized to the lowest masonry courses in the rocking toe region [4]. However, the installation of the post-tensioning tendons complicates construction, and ultimately can lead to poor performance in terms of the wall deformation capacity [5]. In addition, further studies have shown that controlled rocking masonry systems have low inherent damping compared to conventional masonry systems [7]. Such studies demonstrated that while the overall response of a CRMW is desirable, there are still key issues that need to be addressed.

Using DRAIN-2DX [8], a numerical model was developed and validated in [9] using the series of walls tested by Laursen & Ingham [4]. The model contained fibre elements, with the end result of simplifying the analysis to a SDOF equivalent model [9]. This modelling approach vastly underestimated the experimental shear forces by a factor of 2.1 to 2.6, and also failed to capture the corresponding failure modes, particularly those of compression rocking toe failure at high drift

ratios [9]. More recently, Hassanli et al. [7] developed a detailed finite element model using LS-DYNA [10] to conduct a parametric study on various parameters of post-tensioned masonry walls [7]. Notably, this work focused on post-tensioning tendons as a primary factor to generate governing equations that can predict the overall response of post-tensioned CRMWs.

The current study investigates a new CRMW system that avoids the use of post-tensioning. Specifically, the CRMW system relies on gravity loads as restoring forces for self-centering and also uses a supplemental energy dissipation device at the wall base to address the low inherent damping of the system. This energy dissipation device have been developed as part of an ongoing research project at McMaster University [11]. These restoring forces that contribute to the self-centering behaviour are from the self weight and additional dead loads carried by the wall. Figure 1 shows the rocking behaviour and the theoretical hysteretic response of this CRMW system. To facilitate the adoption of this new system within the future editions of the relevant masonry standards, the current study develops a 3D numerical model in OpenSees [12] using multi-layer shell elements to simulate the hysteretic response shown in Figure 1. As very limited data from CRMWs without post-tensioning is available, the model is calibrated against data of CRMW tests that included post-tensioning. The model results are then used to develop a damage index that is validated using the observed damage in the experimental results reported by Hassanli et al. [7]. Finally, the validated model is used to compare the damage experienced in a conventional masonry shear wall compared to the proposed CRMW system with supplemental energy dissipation.

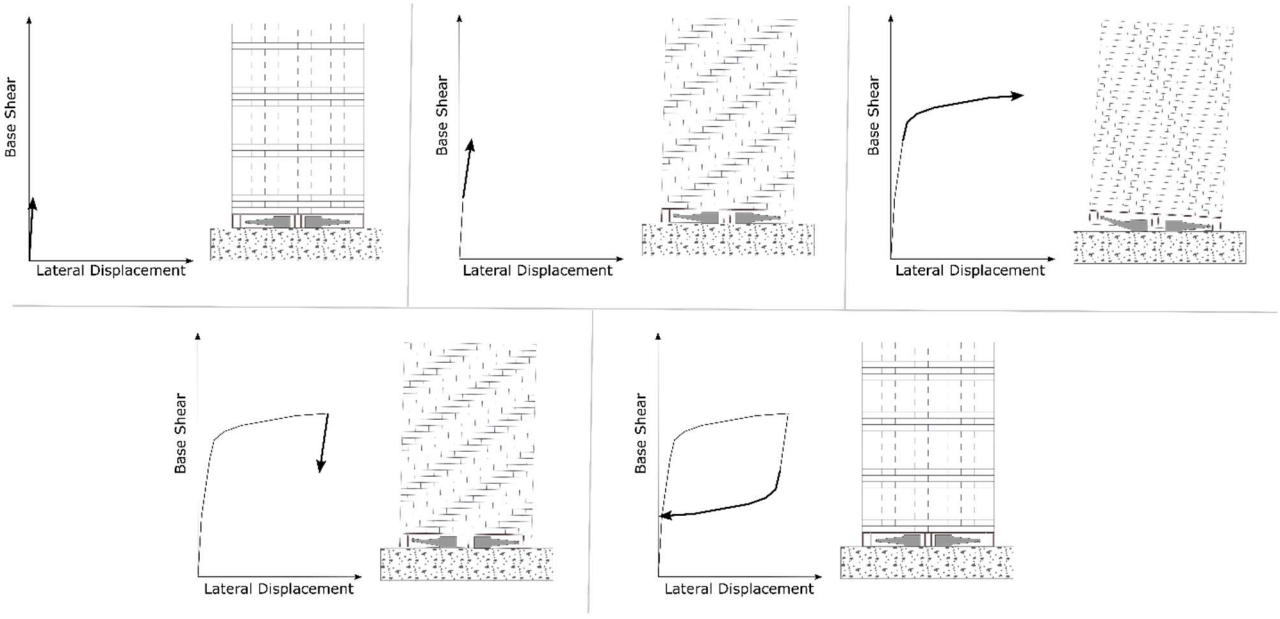

Figure 1: CRMW idealized hysteretic response

NUMERICAL MODEL

Element type

The element used to model the assemblages is based upon work by Dvorkin et al. [13] regarding the theory of mixed interpolation of tensorial components (MITC). The multi-layered shell element was implemented for use in OpenSees [12] by Lu *et al.*. [14] for modelling the seismic response of reinforced concrete shear walls in super tall buildings. The "ShellMITC4" element is a four-node composite element and consists of various layers to simplify the three-dimensional behavior of the composite section into several fully-bonded layers in the thickness direction.

The calculated stresses over a layer of thickness is assumed to be consistent with those at the mid-surface point of that layer, such that the element can predict the stress distribution over the thickness of the wall [14, 15, 16, 17]. Nonlinear material behavior in the form of cracking and aggregate interlocking is incorporated in the planar concrete constitutive material model. In the element, the axial strains and section curvatures are initially calculated in the middle layer, and then the strains of each layer are calculated based on the assumption of plane sections remaining plane. Following the determination of the strains, the stresses in each layer are calculated based on the assigned material model. This element has been proven to be effective at modelling reinforced concrete shear walls, properly capturing the in-plane and out-of-plane bending, as well as direct shear, and coupled bending and shear forces [14, 15, 16, 17, 18].

The rocking interface is modelled with a series of zero length, compression only springs, as shown in Figure 2. The energy dissipation device is connected to the wall at the end node, slaved in the vertical and horizontal degrees of freedom, representative of the pinned connection used for the actual devices.

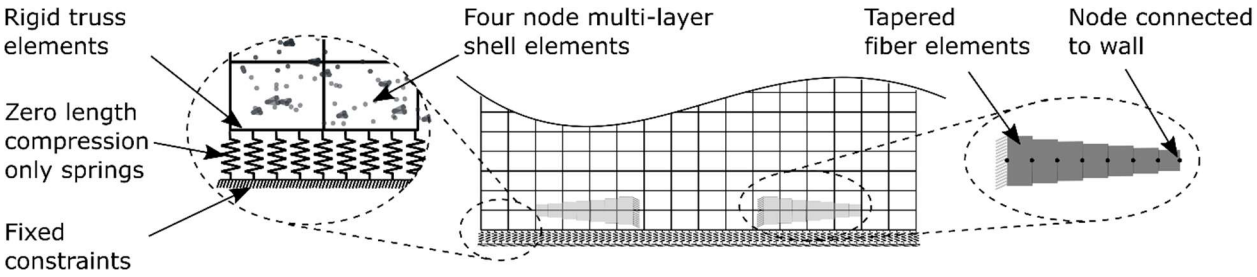

Figure 2: Model schematic

Material models

The masonry fibers within the multi-layered elements are assumed to follow the modified Kent-Scott-Park stress strain model available as Concrete01 in Opensees [12]. It is incorporated using a type of nDMaterial in Opensees – PlaneStressUserMaterial. The parameters specified for the masonry material layers are defined by compressive strength, tensile strength, crushing strength,

strain at maximum strength, strain at crushing strength, ultimate tensile strain and the shear retention factor.

The reinforcing bars are modelled as smeared layers of equivalent thicknesses, designated as *PlateRebar* following the stress strain model referred to as Steel02 (Giuffre-Menegotto-Pinto steel) in OpenSees. The flexural energy dissipation devices are modelled with Steel02, with a low cycle fatigue material property assigned in OpenSees called Fatigue.

Damage index

A damage index introduced by Kim *et al.* [19] is initially calibrated for reinforced concrete structures based on studies of compression and tension failure modes. This damage index has been used in further studies for controlled rocking post-tensioned concrete systems by Jafari *et al.* [20], In the damage index, failure criterion is checked by comparing the principal compressive strains. Modified from the recommendation for reinforced concrete by Kim *et al.* [19] and based on experimental results conducted on confined and unconfined prisms tested in 2019, as well as prior research by Priestley and Elder [21]. As the current study only looks at unconfined masonry, as such, the ultimate compressive strain (ε_{mu}) was taken as 0.003. The compressive damage index (DI_c) is then defined by Kim *et al.* [19] based on this ultimate compressive strain, and the masonry strains (ε_m) obtained from the analysis, as well as a fatigue parameter f_{tg} as:

$$DI_C = 1 - f_{tg}\left[\frac{2\varepsilon_{mu} - \varepsilon_m}{2\varepsilon_{mu}}\right]^2 \tag{1}$$

The fatigue parameter, f_{tg}, is defined as:

$$f_{tg} = 1 - 0.3 b_c \tag{2}$$

Where b_c is defined as the accumulated fatigue damage of masonry based on the number of complete cycles to failure (N_{fc}).

$$b_c = \sum_{i-1}^{n} \frac{1}{N_{fc_i}} \tag{3}$$

$$\log\frac{N_{fc}}{k_c} = \begin{cases} \dfrac{1}{b_c}\left[1 - \dfrac{\left(\varepsilon_m - \varepsilon_{min}\right)^2 - \left(\varepsilon_m - \varepsilon_{max}\right)^2}{\left(\varepsilon_m - \varepsilon_{min}\right)^2}\right] & \varepsilon_{max} < 0.7\varepsilon_m \\ \dfrac{0.09\varepsilon_{mu}}{\varepsilon_{mu} - 0.7\varepsilon_m}\dfrac{1}{b}\dfrac{\varepsilon_{max} - \varepsilon_{min}}{\varepsilon_m - \varepsilon_{min}} & \varepsilon_{max} \geq 0.7\varepsilon_m \end{cases} \tag{4}$$

where $\varepsilon_{max/min}$ are the maximum and minimum cyclic strains obtained up until that point in the analysis, b is a material constant assumed as 0.0588, and k_c is defined as:

$$k_c = 2\frac{f'_{mconfined}}{f'_{munconfined}} \quad (5)$$

The current study only examines unconfined masonry (with k_c being set to 2), but the damage index used allows for the influence of confinement to be captured in future studies. In addition to the compressive damage index proposed by Kim *et al.* [19], a tensile DI was also incorporated in this analysis to capture shear cracks and tensile splitting damage effects. The tensile DI is defined as follows, with ε_{mtu} being defined as the peak tensile strain, assumed to be 0.0002:

$$DI_T = 1 - \left[\frac{2\varepsilon_{mtu} - \varepsilon_{mt}}{2\varepsilon_{mtu}}\right]^2 \quad (6)$$

The damage index for each element was taken as the larger of the DI_T and DI_c.

MODEL VALIDATION

The numerical model developed in the current paper was validated against two CRMWs tested by Hassanli *et al.* [7]. The details of the post-tensioned CRMWs used for validation are summarized in Table 1. Figure 3 shows that there is good agreement between the experimental hysteresis loops and the corresponding results from the OpenSees model.

Table 1 – Summary of wall dimensions and PT details

Specimen	Thickness (m)	Length (m)	Height (m)	Number of PT bars	PT bar spacing (m)	PT initial force (kN)	PT Area (mm^2)	Initial axial stress (MPa)
W2	0.19	1.4	2.3	3	0.6	120	942	1.35
W3	0.19	1.4	2.3	4	0.4	90	1256	1.35

The damage index was validated against the results published by Hassanli *et al.* [7]. The shear, compressive and tensile strains of each element were recorded for each load step and used to obtain the principal strains. Equations 1 and 6 were then used to calculate the damage index for each element at each load step of the analysis. Ultimately, the highest value for each element was taken and plotted on the surface of the model and compared to reported damage from the experimental work in Figure 4. As shown in Figure 4, the damage index captures the initiation of crushing at the wall toes, as well as the development of diagonal shear cracks at the end of the tests. It is important to note that limited photos of the damage observed during these tests were available in the cited material. The exact location of the diagonal cracks observed in the damage index model are different than those observed in the test itself, due to the idealized nature of the smeared multi-layered shell elements used. In the test, the cracks start at one face joint and propagate through the joints, whereas in the model the cracks are seen spreading at a clearer 45-degree angle from the rocking corners of the wall. The initiation of the cracks and the extent of shear cracking observed

in the damage index model are consistent with the observed damage in the reference wall, however more validation of the diagonal shear crack damage index is required in future research.

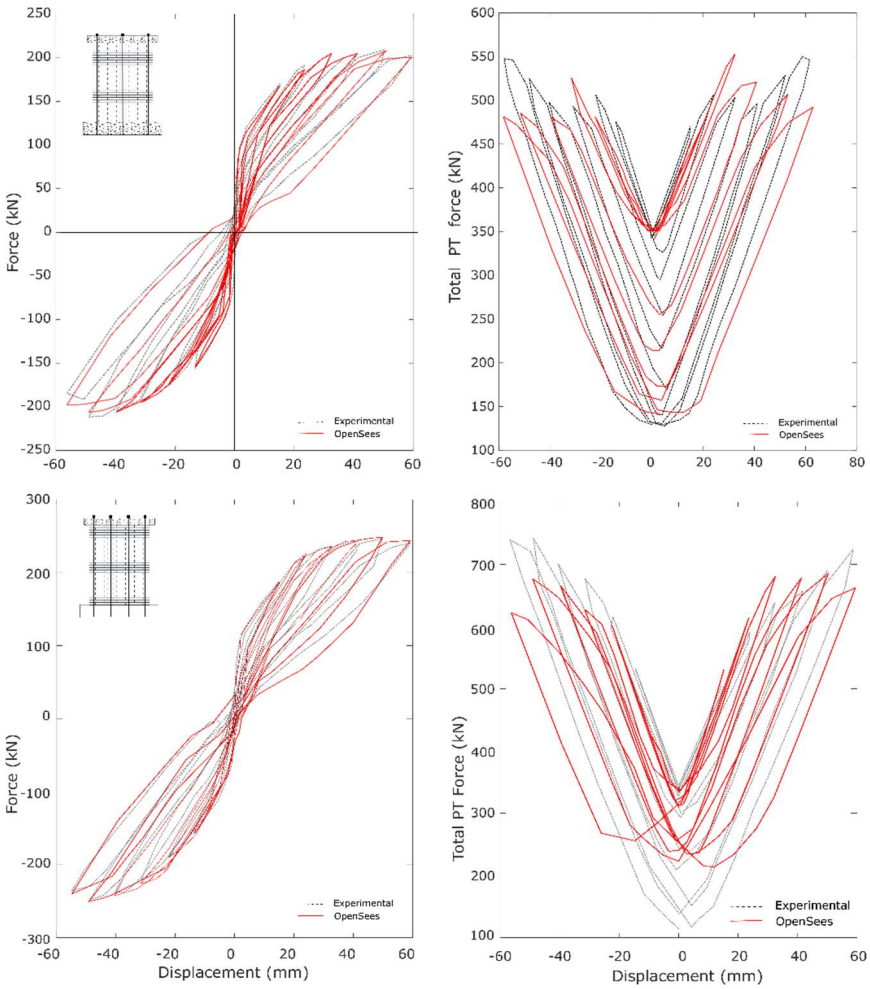

Figure 3: Experimental and Numerical hysteresis loops and PT Force of W2 and W3

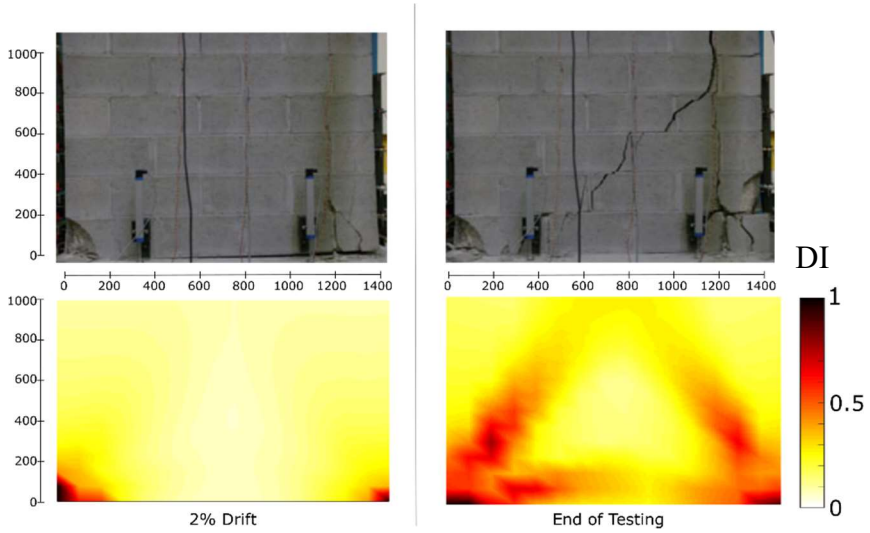

Figure 4: Damage Index validation of W3 (top photos from [7])

Energy Dissipation Device

The current study aims at capturing the response of a CRMW with flexural yielding devices affixed at the base of the wall, as shown in Figure 1. These devices have been developed as part of an ongoing research project at McMaster University [11]. The flexural yielding energy dissipation devices were modelled using tapered fiber elements and validated against a series of experimental tests [11]. A thorough explanation on the experimental work as well as model development and validation can be found in [11].

ANALYSIS

Archetype Walls

Two models were developed in this paper, one representing a conventional ductile reinforced masonry shear wall and another representation a CRMW with flexural energy dissipation devices affixed at the base. The CRMW was designed using a modified set of equations proposed by Hassanli et al. [7] with replacing the post-tensioning terms with design equations for the flexural arm devices [11]. Figure 5 shows the results of a displacement-based pushover analysis obtained from each archetype wall, done by displacing the central roof node.

The details of each wall are summarized in Table 2. The flexural arm used in the CRMW was designed in order to give a comparable hysteretic response to the fixed base wall using design equations found in [11]. As the gravity load is necessary for the behaviour of the proposed CRMW, the designed gravity load is larger in the CRMW, within a reasonable range of 0.15 f'm, as shown in Table 2. This increased gravity load comes from larger self-weight and dead loads on the CRMW.

Table 2: Summary of wall dimensions and PT details

Specimen	Thickness (mm)	Length (mm)	Height (mm)	r_v (%)	r_h (%)	f_y (MPa)	Axial stress (MPa)	f'_m (MPa)
CRMW	203	3710	6096	0.82	1.27	420	3.15	21
Fixed Base (FB)	203	3710	6096	0.82	1.27	420	1.47	21

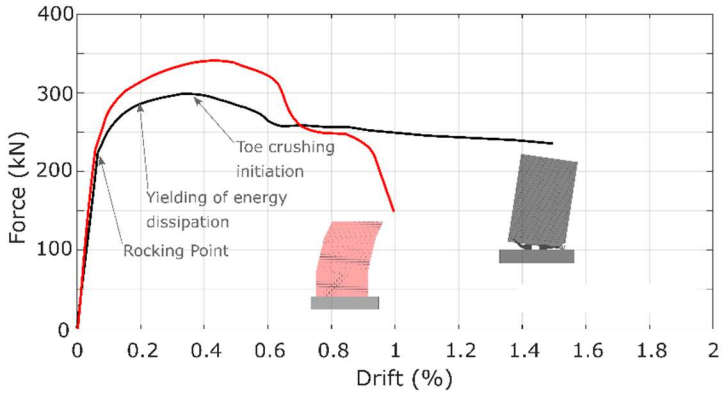

Figure 5: Archetype pushover curves

The fixed base wall was simulated until a drift of 1%, at which it has lost over 50% of its peak lateral force. The CRMW was simulated until a drift of 1.5%.

ANALYSIS RESULTS

Figure 6 shows the results of a cyclic pusover conducted on each wall and the damage observed at drift levels of 0.5% and 1%. There is considerably more damage observed in the fixed base wall, particularly in the base of the wall, designed as the plastic hinge region. This region has extentive crushing occur as well as tension cracks appearing even at the low drift of 0.5%. The CRMW conversely, has an isolated amount of damage concentrated at the rocking toe portion of the wall, as well as at the anchor point of the flexural arm energy dissipation device.

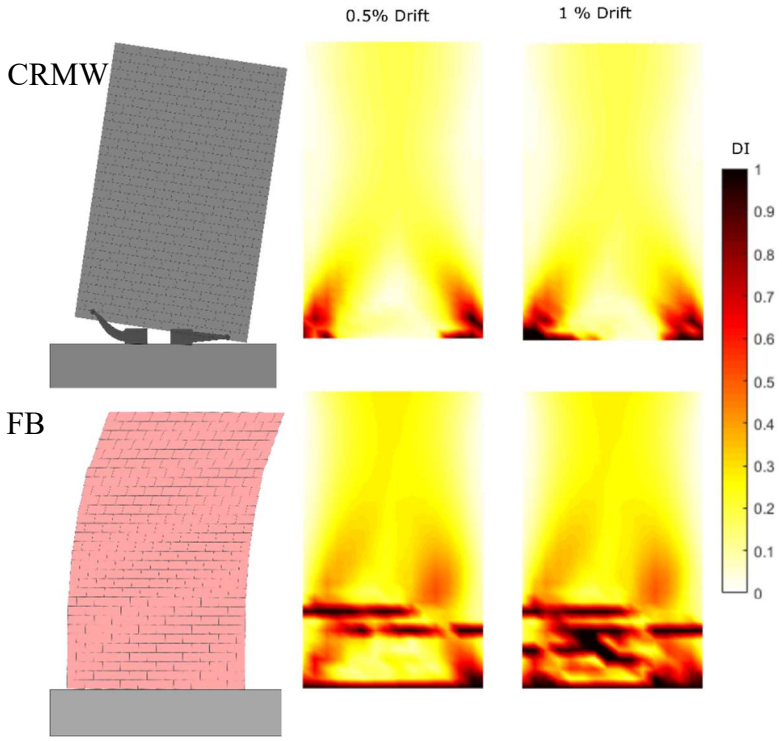

Figure 6: Damage index at different drift levels comparison

Damage states

Prior studies incorporating this damage index approach to damage quantification for reinforced concrete controlled rocking walls indicated damage levels associated with particular DI values [20]. A value of 0.1 is attributed to minor damage, a value of 0.4 is attributed to repairable damage, whereas a damage ratio exceeding 0.7 is irreparable severe damage [20]. It should be noted that this study included a tensile damage index in addition to the compressive damage index found in [20].

Figure 7 shows the area of the wall reaching each of these damage states at increasing drifts. It is apparent that the CRMW undergoes significantly less damage while withstanding a larger gravity load, experiencing higher drift, and experiencing less strength degradation.

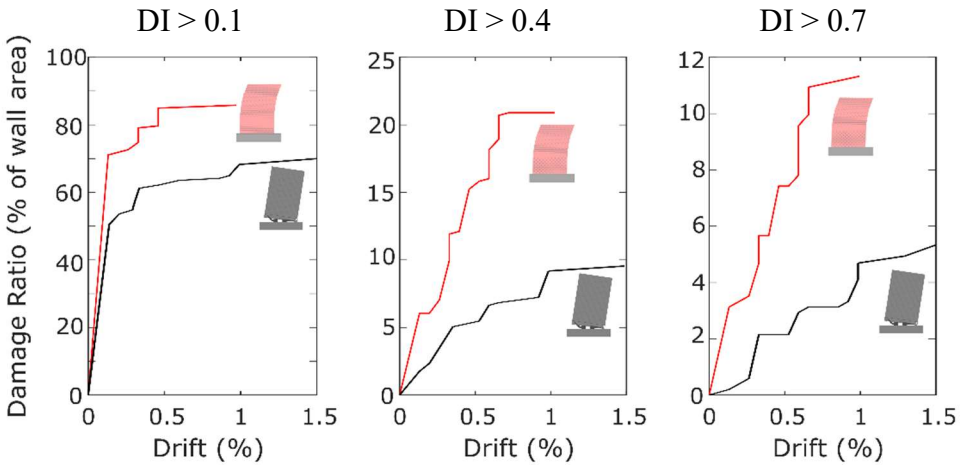

Figure 7: Damage ratios as a percentage of total wall area

CONCLUSION

This study presented the development and validation of a new technique for modelling controlled rocking masonry shear walls. The shell elements used can capture detailed information at the element level that was associated with a damage index. The damage index was validated against existing experimental tests. The validated model was then used to simulate a new innovative CRMW in comparison to a comparable conventional masonry shear wall. The results of the study indicated that the proposed CRMW design incorporating flexural energy dissipation devices is promising and is expected to experience significantly less damage than a conventional masonry shear wall. Experimental work is required to further validate the numerical model as well as better understand the proposed system of a CRMW without post-tensioning and with additional flexural energy dissipation devices attached at the base.

ACKNOWLEDGEMENTS

This study was supported by the Canada Masonry Design Center (CMDC), the Canadian Concrete Masonry Producers Association (CCMPA), the National Science and Engineering Research Council of Canada (NSERC), and the Ontario Centers of Excellence (OCE).

REFERENCES

[1] R. Eguchi, J. Goltz, C. Taylor, S. Chang, P. Flores, L. Johnson, H. Seligson and N. Blais, "Direct economic losses in the Northridge earthquake: A three-year post-event perspective," *Earthquake Spectra,* vol. 14, no. 2, pp. 245-264, 1998.

[2] J. M. Ingham, D. T. Biggs and L. M. Moon, "How did unreinforced masonry buildings perform in the February 2011 Christchurch earthquake?," *Structural Engineer,* vol. 89, no. 6, pp. 14-18, 2011.

[3] ACI Innovation Task Group 5, Requirements for Design of a Special Unbonded Post-tensioned Precast Shear Wall Satisfying ACI ITG-5.1 and commentary, American Concrete Institute, 2009.

[4] P. T. Laursen and J. M. Ingham, "Structural Testing of Large-Scale Posttensioned Concrete Masonry Walls," *Journal of Structural Engineering,* vol. 130, no. 10, pp. 1497-1505, 2004.

[5] O. A. Rosenboom and M. J. Kowalsky, "Reversed in-plane cyclic behavior of posttensioned clay brick masonry walls," *Journal of Structural Engineering,* vol. 130, no. 5, pp. 787-798, 2004.

[6] G. D. Wight, Seismic performance of a post-tensioned concrete masonry wall system, Aukland: The University of Aukland, 2006.

[7] R. Hassanli, M. A. ElGawady and J. E. Mills, "In-plane flexural strength of unbonded post-tensioned concrete masonry walls," *Engineering Structures,* pp. 245-260, 2017.

[8] V. Prakash, G. Powell and S. Campbell, "DRAIN-2DX Base Prcgram Description and User Guide," Department of Civil Engineering, University of California, Berkeley, Berkeley, 1993.

[9] P. Laursen, Seismic analysis and design of post-tensioned concrete masonry walls (Doctoral Dissertation), Retrieved from : http://researchspace.auckland.ac.nz/feedback, 2002.

[10] Livermore Software Technology Corporation, "LS DYNA," LSTC, 1978.

[11] J. Li, *Development of a flexural yielding energy dissipation device for controlled rocking masonry walls,* MASc Thesis: McMaster University, 2019.

[12] F. M. M. H. S. G. L. F. Silvia Mazzoni, OpenSees Command Language Manual, Pacific Earthquake Engineering Research (PEER) Center, 2006.

[13] E. N. Dvorkin, D. Pantuso and E. A. Repetto, "A formulation of the MITC4 shell element for finite strain elasto-plastic analysis," *Computer methods in applied mechanics and engineering,* pp. 17-40, 1995.

[14] X. Lu, L. Xie, H. Guan, Y. Huang and X. Lu, "A shear wall element for nonlinear seismic analysis of super-tall buildings using OpenSees," *Finite Elements in Analysis and Design,* pp. 14-25, 2015.

[15] H. Guan and Y.-C. Loo, "Flexural and shear failure analysis of reinforced concrete slabs and flat plates," *Advances in Structural Engineering,* pp. 71-85, 1997.

[16] P. Hallinan and H. Guan., "Layered finite element analysis of one-way and two-way concrete walls with openings.," *Advances in Structural Engineering ,* pp. 55-72, 2007.

[17] X. Lu, L. Xinzheng, G. Hong and L. Ye, "Collapse simulation of reinforced concrete high-rise building induced by extreme earthquakes," *Earthquake Engineering & Structural Dynamics,* pp. 705-723, 2013.

[18] Z. Miao, Y. Lieping, G. Hong and L. Xinzheng, "Evaluation of modal and traditional pushover analyses in frame-shear-wall structures," *Advances in Structural Engineering,* pp. 815-836, 2011.

[19] L. K. C. Y. S. H. Kim TH, "Seismic damage assessment of reinforced concrete bridge columns," *Engineering Structures,* vol. 27, no. 4, pp. 576-592, 2005.

[20] D. R. Jafari Abouzar, "Estimation of Load-Induced Damage and Repair Cost in Post-Tensioned Concrete Rocking Walls," *Journal of Shanghai Jiaotong University,* vol. 23, no. 1, pp. 122-131, 2018.

[21] M. J. N. Priestley and D. M. Elder, "Stress-Strain Curves for Unconfined and Confined Concrete Masonry," *ACI Journal,* pp. 192-201, 1983.